Proceedings

of the

4th International Modal Analysis Conference

Los Angeles, CA

1986

Volume II

Union College,
Schenectady, N.Y. 12308

VIRTUAL COHERENCE: A DIGITAL SIGNAL PROCESSING TECHNIQUE FOR INCOHERENT SOURCE IDENTIFICATION

S.M. Price[1] and R.J. Bernhard
School of Mechanical Engineering
Ray W. Herrick Laboratories
Purdue University
West Lafayette, Indiana 47907

ABSTRACT

The digital signal processing techniques for identification of noise or vibration energy sources; ordinary, multiple and partial coherence techniques, either require incoherence of the measured input data or a degree of *apriori* knowledge of the system. This paper discusses a transformation technique for conditioning the measured spectra to determine how many real incoherent sources exist and to create a virtual image of those sources at the measurement plane. In addition, the conditioned spectra can be used to generate a "virtual" coherence function between the measured output and each of the incoherent inputs.

INTRODUCTION

Coherence functions are potentially very attractive for energy source identification [1]. Attributing percentage of output energy to individual measured system inputs permits a ranking of sources and, hopefully, reasonable insight into the efficient solution of dynamic problems. Practically, however, coherence techniques are limited by several factors. In most real machinery, either the real sources are unknown or cannot be measured directly. Thus, measurements usually occur somewhere in the energy transmission path where they are often contaminated by energy from all the sources. Secondly, coherence techniques are derived for non-deterministic signals, only. Deterministic signals, whether generated by the same source or not, will appear to be coherent. Since sources in machinery tend to operate synchronously with machine speed, the measured inputs may be largely deterministic, and hence, mutually coherent.

The multiple coherence function gives an estimate of measurement noise at the output which is not coherent with any of the inputs. When there is no coherence between inputs a multiple coherence can be used to attribute parts of the coherent output energy to particular inputs. However, when coherence exists between inputs, other techniques must be used to distribute energy sources. Partial coherence techniques are used to attribute energy from particular inputs to the output given a specific system model. However, for realistic machinery systems this model is not well known *apriori* and furthermore, numerical error becomes a significant factor for systems with large numbers of inputs. The utility and limitations of coherence functions have been demonstrated by a great number of investigators [2-6].

This paper discusses a linear transformation technique which will condition the measured input spectra to identify how many incoherent sources exist. The technique will compute a frequency spectrum of each incoherent source which is an image of the real source. A coherence function is also generated which apportions the output energy due to each incoherent source. This function is referred to as virtual coherence in this paper [7]. Some similar conditioning, referred to as latent root extraction, is done on correlation functions by Jenkins and Watts [8]. The virtual coherence function is robust in that no *apriori* knowledge of the system is required nor is it necessary to measure at the energy input point in order to determine a valid coherence function.

THEORY

A noiseless single input, single output system can be described mathematically by

$$S_y(f) = |H(f)|^2 S_x(f) \tag{1}$$

where $S_y(f)$ is the power spectral density of the output, $S_x(f)$ is the power spectral density of the input, and H(f) is the frequency response function. In an actual system, some noise may be present in the output. The ordinary coherence function

$$\gamma^2 = \frac{|S_{xy}(f)|^2}{S_x(f)S_y(f)} \tag{2}$$

has been formulated to indicate the noise at the output that is not present at the input. For a system with no noise, the ordinary coherence function is unity. A system contaminated with some noise will have coherence $0 \leq \gamma^2 \leq 1$. If the ordinary coherence function is much less than unity, (say .8 or less) the system should be modeled as having more than one input, and a multiple input, single output formulation should be used.

For the multiple input, single output system depicted in Fig. 1, the input vector in the frequency domain is,

$$\bar{x}^T(f) = [x_1(f), x_2(f), \cdots, x_n(f)] \tag{3}$$

where $x_1, \cdots, x_n$ are the inputs. The frequency response function (FRF) vector is

$$\bar{H}^T(f) = [H_1(f), H_2(f), \cdots, H_n(f)] \tag{4}$$

where $H_1, \cdots, H_n$ are the FRF's for each input. An n x n dimensional cross spectral density matrix can be written

1 Currently at Engineering Dynamics Inc., San Antonio, TX.

$$\underline{S}_{xx}(f) = \begin{bmatrix} S_{11} & S_{12} & \cdots & S_{1n} \\ S_{21} & S_{22} & \cdots & S_{2n} \\ . & . & & . \\ . & . & & . \\ . & . & & . \\ S_{n1} & S_{n2} & \cdots & S_{nn} \end{bmatrix} \quad (5)$$

where the diagonal terms are the power spectral densities (PSD's) of each input, and the off diagonal terms are the cross spectral densities (CSD's) between pairs of inputs. For a system in which the inputs are completely incoherent, the CSD terms will be zero, making the $\underline{S}_{xx}$ matrix diagonal.

The output power spectral density S_{yy} can be expressed by,

$$S_{yy}(f) = \bar{H}^H(f)\, \underline{S}_{xx}(f)\, \bar{H}(f) \quad , \quad (6)$$

where the superscript H denotes the hermitian transpose of the vector or matrix it modifies. An overbar is used here to indicate a vector, and an underbar indicates a matrix. Symbols that are not annotated are scalers. For simplicity, the (f) denoting a function of frequency will be dropped from the notation with the understanding that there is a separate matrix equation of the form of Eq. 6 at each discrete frequency.

The cross spectra between the inputs and the output is described by,

$$\bar{S}_{xy} = \underline{S}_{xx}\, \bar{H} \quad , \quad (7)$$

where $\bar{S}_{xy}$ is the vector whose elements are the cross spectra between each input and the output, y.

A form of the coherence function suitable for a multiple input system can be developed from Eq. 6

$$\gamma^2_{x:y} = 1 - \frac{|S_{yxx}|}{S_{yy}\, |\underline{S}_{xx}|} \quad ,$$

The matrix $\underline{S}_{yxx}$ is obtained by augmenting the CSD matrix with a row and a column consisting of the $\bar{S}_{xy}$ vector, and the PSD of the output, S_{yy}. When the inputs are mutually incoherent, $S_{ij} = 0$ $(i \neq j)$ the multiple coherence function decomposes to a sum of ordinary coherences.

$$\gamma^2_{x:y} = \gamma^2_{1:y} + \cdots + \gamma^2_{n:y} \quad (8)$$

or,

$$\gamma^2_{x:y} = |H_1|^2 S_{11} + \cdots + |H_n|^2 S_{nn} \quad (9)$$

The individual terms in Eqs. 8 or 9 represent the ratio of output energy due to each input.

If any coherence exists between inputs, the multiple coherence function becomes much more complicated than Eqs. 8 or 9 and attributing output energy to a particular source is uncertain. In most realistic situations, there will be at least some coherence between inputs, which limits the usefulness of multiple coherence function in complicated systems.

An alternate formulation, partial coherence, was developed to consider the case of partially coherent inputs [1]. Partial coherence requires the investigator to identify which measured input is the primary source of the coherent signal. The partial coherence technique removes the linear interdependence between inputs by conditioning the input signals. Partial coherence is computed using these conditional inputs. The partial coherence function indicates how much of the output energy is due to the coherent signals identified with a particular source.

In order to obtain meaningful values for ordinary coherence, the model used for computing partial coherences must be ordered in a very particular fashion. Specifically, the mth input, $x_m(t)$ can only be partially coherent with sources $x_1(t)$ to $x_{m-1}(t)$. All other sources, $x_{m+1}(t)$ to $x_n(t)$ must be incoherent with $x_m(t)$. For complicated systems, the information necessary for proper ordering is usually not known. Furthermore, when two or more inputs are perfectly coherent with each other numerical problems occur. As a practical restriction, the number of measured inputs must not be significantly greater than the number of incoherent sources or numerical problems result from the conditioning operation on the inputs. A new technique is thus necessary which is more robust and can describe a system in which all inputs are partially or fully coherent with each other and where the properties of the signals are largely unknown.

Mathematical techniques exist that will remove linear dependence between elements without having to order the system in a particular manner [9]. Specifically, a system existing in n dimensional space, with rank m $(m \leq n)$ can be transformed by a linear transformation to a system of dimension m (e.g., a plane in 3-space). Thus, a system that has n measured inputs, but has only m incoherent source mechanisms can be reduced by linear transformation to generate a set of incoherent "virtual" inputs. A model of such a system is shown in Fig. 2 where u' is the real source and x' is an image of the real source or virtual source. The CSD matrix, $\underline{S}_{xx}$ may be diagonalized by a linear transformation of the form.

$$\underline{S}_{xx}' = \underline{P}^H\, \underline{S}_{xx}\, \underline{P} \quad , \quad (10)$$

where $\underline{P}$ is a unitary matrix formed by writing the eigenvectors of $\underline{S}_{xx}$ as columns, and $\underline{S}_{xx}'$ is the diagonal matrix of eigenvalues of $\underline{S}_{xx}$. The properties of the Hermitian transformation, also allow Eq. 10 to be rewritten as

$$\underline{S}_{xx} = \underline{P}\, \underline{S}_{xx}'\, \underline{P}^H \quad , \quad (11)$$

Substituting 11 into 7 yields

$$\underline{P}^H\, \bar{S}_{xy} = \underline{S}_{xx}'\, \underline{P}^H\, \bar{H} \quad , \quad (12)$$

If $\underline{P}^H\, \bar{S}_{xy}$ is defined to be the virtual cross spectra vector, $\bar{S}_{xy}'$, $\underline{P}^H\, \bar{H}$, is defined to be the virtual FRF vector, $\bar{H}'$, Eq. 12 can be rewritten as,

$$\bar{S}_{xy}' = \underline{S}_{xx}'\, \bar{H}' \quad , \quad (13)$$

Since $\underline{S}_{xx}'$ is diagonal, the virtual FRF vector can be found without inverting $\underline{S}_{xx}'$.

$$H_i' = \frac{S_{iy}'}{S_{ii}'} \quad i=1,2, \cdots n \quad , \quad (14)$$

To obtain a formulation of the coherence function in terms of the virtual spectra, Eq. 11 is substituted into Eq. 6 giving S_{yy} in terms of the virtual inputs.

$$S_{yy} = \bar{H}^H\, \underline{P}\, \underline{S}_{xx}'\, \underline{P}^H\, \bar{H} \quad (15)$$

Further manipulation will result in a formulation of S_{yy} in terms of the virtual spectra.

$$S_{yy} = \bar{H}'^H\, \underline{S}_{xx}'\, H' \quad , \quad (16)$$

Since S_{xx}' is diagonal, Eq. 16 can be rewritten as,

$$S_{yy} = \sum_{i=1}^{n} \left|H_i'\right|^2 S_{ii}' \quad . \tag{17}$$

Dividing through by S_{yy} produces the virtual coherence function,

$$1 = \sum_{i=1}^{n} \frac{\left|H_i'\right|^2 S_{ii}'}{S_{yy}} \quad , \tag{18}$$

which can be rewritten as

$$\gamma^2_{x:y} = \sum_{i=1}^{m} \gamma^2_{x_i':y} \tag{19}$$

$$= \sum_{i=1}^{m} \frac{\left|S_{iy}'\right|^2}{S_{ii}' S_{yy}}$$

where m is the number of incoherent inputs, and $\gamma_{x'_i:y}$ is the ordinary coherence for each virtual input.

The virtual coherence derivation indicates that an arbitrary system of n inputs can be reduced to a system of m $(m \leq n)$ virtual inputs. Furthermore, the contribution that each virtual input (and hence, each real input) has on the output can be computed. Virtual coherence is thus valuable for use in source identification studies. It should be possible to obtain data from transducers monitoring a system, and determine the number of incoherent source mechanisms that are present. Computing the virtual coherence functions will indicate which of the incoherent source mechanisms are producing the signal measured at the output. Although the development shown here does not include the effects of output noise, the virtual coherence function indicates the presence of noise when the value of $\gamma^2_{x:y} < 1$. This indicated noise may be noise signals at the output or may represent sources which are not sensed by any of the transducers.

RESULTS WITH SYNTHETIC DATA

Synthetic data for four system configurations were generated on the computer to test the virtual coherence techniques for typical applications. The first used a two degree-of-freedom system with and without noise at the output. The second and third studies were selected to investigate the effect of deterministic signals.

The system schematic shown in Fig. 2 represents a system from which measured data from 3 transducers is used to describe the energy from a system which has only two incoherent noise generation mechanisms. Using a model of a 2-DOF system, and 2 incoherent sets of random data, (one set of higher amplitude than the other) the data was generated to represent the system of Fig. 2. Physically, this might be a machine instrumented with three transducers on some internal mechanism, and a microphone measuring the sound energy emitted from the machine.

When analyzed, the 3 input, single output system should produce 2 incoherent inputs. There should be two non-zero virtual coherence functions. Furthermore, since the first input was greater in magnitude than the 2nd, the virtual coherences should indicate that one virtual input has a slightly greater effect on the output than the other. Finally, since there is no noise in the output of the signal that isn't in the inputs, the total coherence (the sum of the virtual coherences) should be unity.

Figure 3 is typical of the power spectral density (PSD) of the inputs, and the output. Figures 4-6 show the virtual sources computed from the data. G_{11}' and G_{22}' are clearly two incoherent sources while G_{33}' is very close to zero over the entire frequency range, indicating that there are 2 incoherent source mechanisms present in the system.

Figure 7 shows the virtual coherences for the inputs. Note that since there are only 2 incoherent inputs, $\gamma_{x_1:y}$ is the reflection of $\gamma_{x_2:y}$, and $\gamma_{x_3:y}$ is zero.

The coherence function will also give an indication of any noise that may be present in the output, but not present in any of the inputs. The same test was repeated, but with incoherent noise (i.e., incoherent with the random excitation used to generate the inputs) added to the output. Since the inputs were not altered, the original CSD matrix, and thus the virtual sources, remained unchanged. The total coherence was less than unity, indicating the noise present at the output.

The drop in coherence at the resonance frequencies is an artifact of the way in which the synthetic data was generated. The data was obtained by finding the response of an undamped 2-DOF system, excited by random input. At the resonance frequencies, the numerical model produces nearly deterministic output.

The tests so far indicated that the virtual coherence technique works for systems where purely random signals are present. Since a real system is likely to have some deterministic sources, (i.e., a source whose characteristics at some future time can be predicted) two more studies were conducted using a deterministic signal as at least one of the inputs. A system consisting of 2 deterministic inputs was generated. Virtual coherence analysis showed that only 1 incoherent source was present. The data indicates, as it should, that the virtual source technique does not separate deterministic signals.

Another system consisting of one random input and a harmonic, decaying sine wave (a deterministic input) was generated. The virtual sources computed from the random/deterministic data are shown in Figs. 8 and 9 and indicate that there are clearly two incoherent sources present. At low frequency, the random noise dominates the output signal, while at high frequencies, the decaying sine wave predominates. The virtual coherences are shown in Figs. 10 and 11. At low frequencies where the random input dominates the 1st virtual source, there are drops in virtual coherence at the harmonic peaks. At higher frequencies, the virtual coherence function has peaks at the same frequencies as the harmonic peaks. The reverse is true of the virtual coherence of the 2nd virtual input.

EXPERIMENTAL RESULTS

Experimental data were collected to further test the virtual coherence technique. Experimental data from the system of Fig. 2 was obtained using one random noise generator connected to two speakers and another random noise generator connected to a third speaker. Voltages at each speaker were used as the three measured inputs. The measured output was obtained from a microphone, placed in front of the speakers.

The results should indicate that there are two incoherent sources present in the system. Since one of the random noise sources exhibited a higher amplitude than the other, the virtual coherences should indicate that the output is composed primarily of one of the virtual sources. At low frequencies, the response of the speaker falls off, so background noise may be a significant part of the output. Therefore, the total coherence at low frequencies may be low.

The virtual sources computed indicate that there are only 2 virtual sources present in the system. The virtual coherences, shown in Figs. 12-14 also behave as expected, indicating that one source dominates the other. At low frequencies, the total

coherence (Fig. 15) is low, indicating that some background noise is contaminating the measured response.

A hermetic, reciprocating compressor was instrumented to evaluate the usefulness of the virtual coherence technique in more realistic systems. Four of the possible energy transmission paths were instrumented so that the incoherent source generation mechanisms could be measured. To measure the gas cavity transmission path, a pressure transducer was installed inside the shell, at the top. The path through the oil was measured by a pressure transducer placed in the oil. An accelerometer placed on a suspension spring and an accelerometer placed on the discharge tube measured the mechanical transmission paths. These four transducers provided all of the measured inputs. The instrumented compressor was then placed in the anechoic room and operated at normal conditions. The measured output, shown in Fig. 16, was the radiated sound pressure measured with a microphone.

Data from the pressure transducers was relatively flat as a function of frequency past the first few orders of rotation. Data from the accelerometers showed more response at the higher frequencies. The measured output exhibits the broad peak at 1200 Hz typical of a structural mode of the compressor shell.

The virtual coherence functions (Figs. 17-20) indicate that most of the energy at the output comes from the first two incoherent sources. However, at some frequencies, the 3rd and 4th incoherent sources contribute a good portion of the energy. The total coherence function shown in Fig. 21 indicates that at low frequencies, between the harmonic peaks, a large portion of the energy in the output is not being transmitted through the four measured paths. At higher frequencies, most of the energy at the output consists of the energy present from the four virtual sources. The typical engineering approach would be to re-instrument differently perhaps with more transducers to identify the paths and sources.

While the results obtained from the random noise generators were excellent, the results from the compressor are incomplete. It is obvious from the data that more measured inputs should be obtained to completely evaluate the source mechanisms and transmission paths in the compressor. Additional pressure transducers in the cavity, as well as an accelerometer on each suspension spring would be the best locations for additional transducers.

CONCLUSIONS

Several conclusions seem to be apparent from the data presented. It has been shown in the three synthetic data studies that the virtual coherence techniques are useful for determining the number of incoherent random processes in a system, and for providing an indication of the contribution from each process to the output from the system. There are a few caveats, however. Firstly, deterministic signals from more than 1 source will be lumped into a single source. Secondly, the virtual sources are not consistently associated with individual actual sources. This phenomenon results from numerical sorting of the eigenvectors, and can be seen in Figs. 8 and 9. G_{11}' is a composite of the random noise in the low frequency region and the harmonic decaying sine wave in the high frequency region. G_{22}' shows a similar, but reversed behavior.

The signals obtained from the compressor are not completely deterministic. The virtual coherence functions and the total coherence function provides information about the energy being transmitted through the four paths. There is potential for even more information to be provided by using the eigenvectors computed. These eigenvectors may provide an understanding of how the virtual sources relate to the actual sources, and provide a better indication of energy transmitted through individual noise transmission paths.

ACKNOWLEDGMENTS

This research was supported by a grant from the Herrick Foundation and with hardware donations from the Tecumseh Products Co. of Tecumseh, MI. The authors would also like to thank Hovard Vold of SDRC for his advice early in the investigations and Russ Ruhnow of GENRAD for helping collect data.

REFERENCES

1. Bendat, J.S. and Biersol, A.G., *Engineering Applications of Correlation and Spectral Analysis*, New York: John Wiley and Sons, 1980.

2. Crocker, M.J. and Hamilton, J.F., "Modeling of Diesel Engine Noise Using Coherence," SAE Paper No. 790362, 1979.

3. Alfredson, R.J., "The Partial Coherence Technique for Source Identification on a Diesel Engine, "*J. Sound and Vibration*, 55(9), 487-494, 1977.

4. Chung, J.Y., Crocker, M.J., and Hamilton, J.F., "Measurement of Frequency Responses and the Multiple Coherence Function of the Noise-Generation System of a Diesel Engine, "*J. Acoustical Society of America*, 58(3), 635-642, 1975.

5. Tretheway, M.W., Evenson, H.A., and Shapton, W.R., "Combination of Multiple Input Models and Experimental Modal Analysis for Identification of Structural Noise Generating Mechanisms with Applications to Forge Hammers, "*Noise Control Engineering Journal*, 21(3), 89-102, 1983.

6. Wagstaff, P.R., and Henrio, J.C., "Identification of Noise Sources in Steam Turbine Plant Using Multiple Input Analysis on a Digital Computer," *Proceedings of Noise Con 85*, 293-297.

7. Price, S.M., "Identification of High Frequency Noise Paths and Noise Source Mechanisms in Reciprocating Hermetic Compressors," M.S. Thesis, Purdue University, 1985.

8. Jenkins, G.M. and Watts, D.G., *Spectral Analysis and Its Application*, San Francisco:Holden-Day, 1968.

9. Noble, B. and Daniel, J.W., *Applied Linear Algebra*, Prentice Hall, 1977.

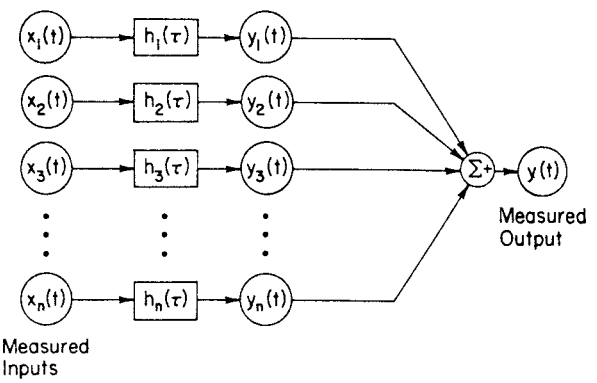

Figure 1. Multiple Input, Single Output Model

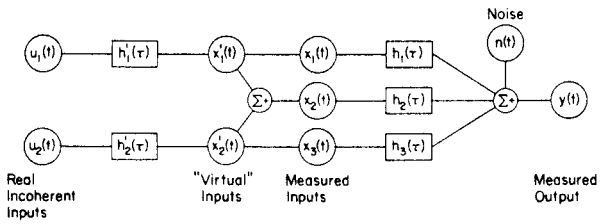

Figure 2. Multiple Input, Single Output Model with Virtual Sources

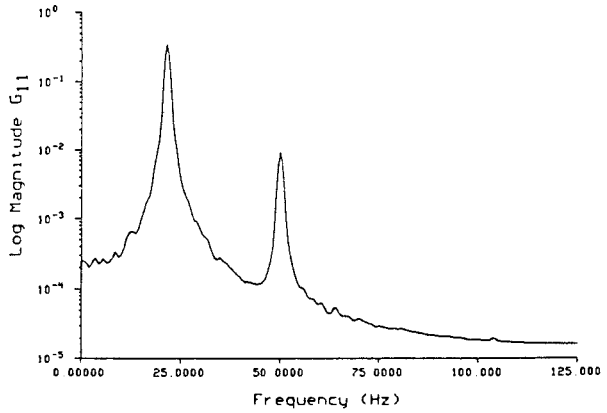

Figure 3. One-Sided PSD of 2-DOF System, Input #1

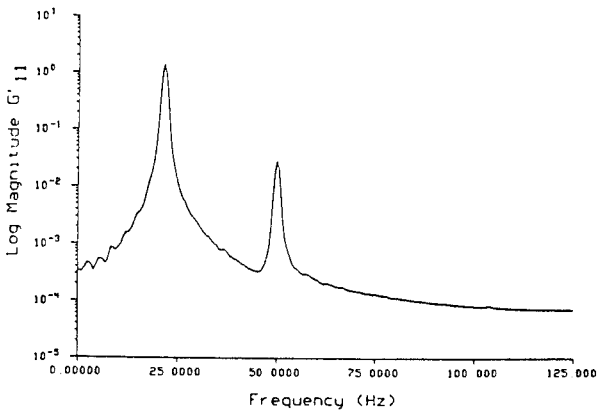

Figure 4. Virtual Source #1 of 2-DOF System

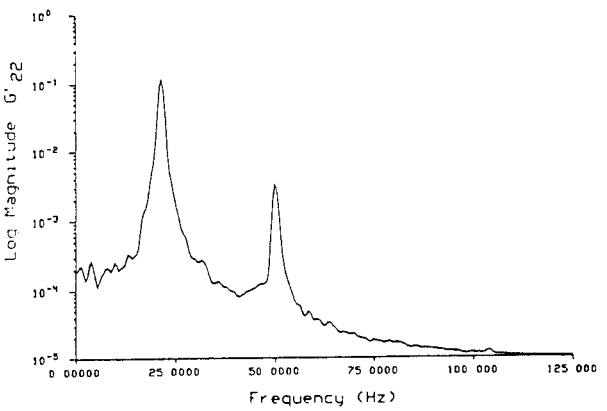

Figure 5. Virtual Source #2 of 2-DOF System

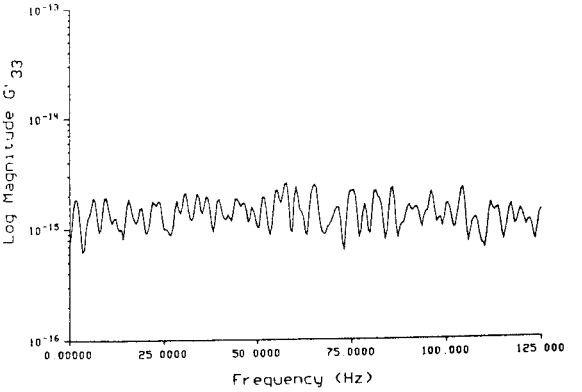

Figure 6. Virtual Source #3 of 2-DOF System

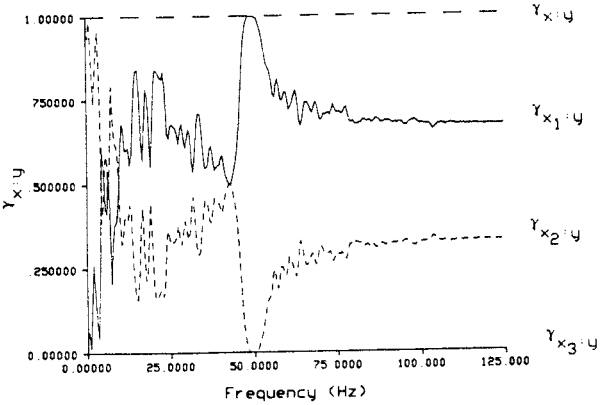

Figure 7. Virtual Coherences for 2-DOF System

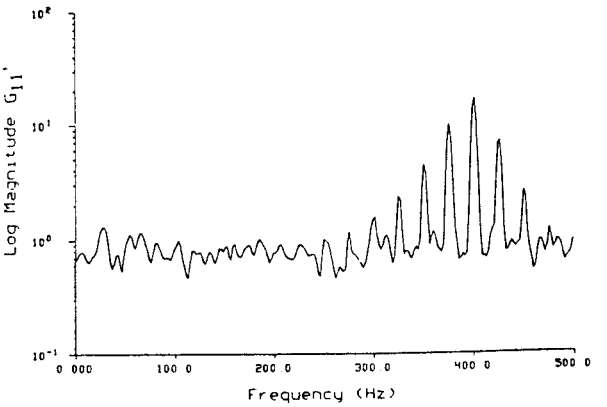

Figure 8. Virtual Source #1 of Random/Deterministic Signals

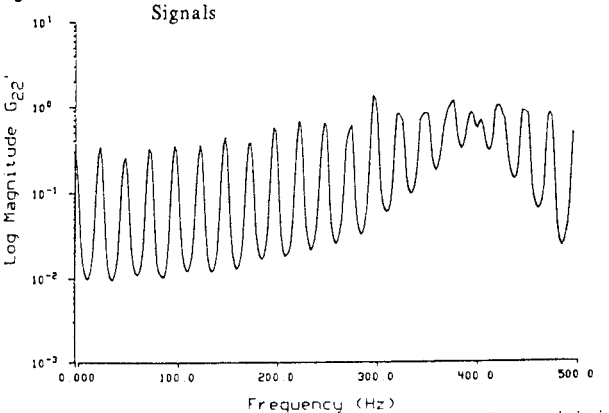

Figure 9. Virtual Source #2 of Random/Deterministic Signals

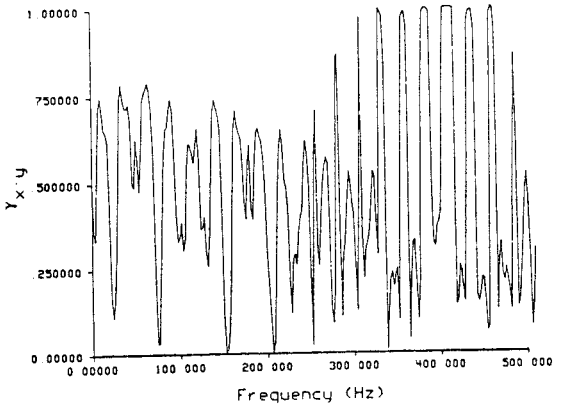

Figure 10. Virtual Coherence #1 of Random/Deterministic Signals

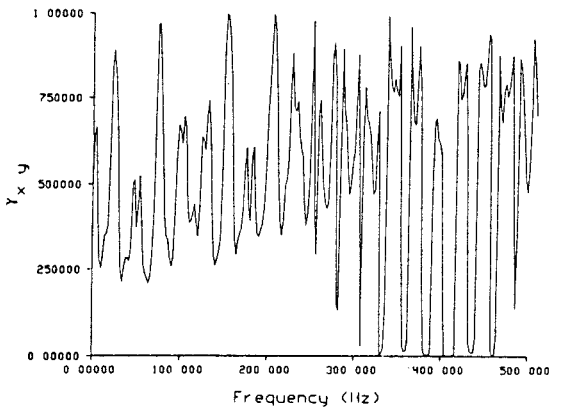

Figure 11. Virtual Coherence #2 of Random/Deterministic Signals

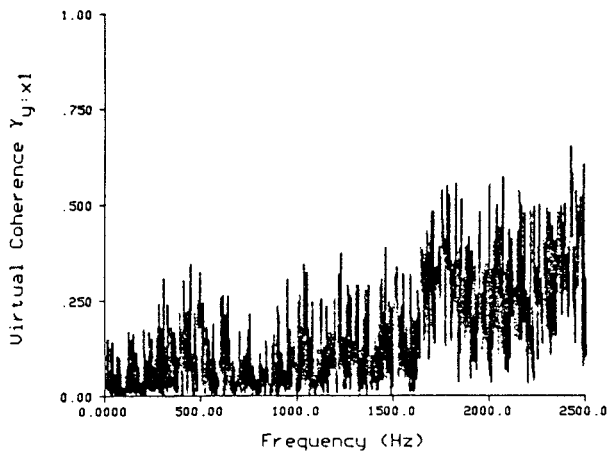

Figure 12. Virtual Coherence #1, Random Noise Test

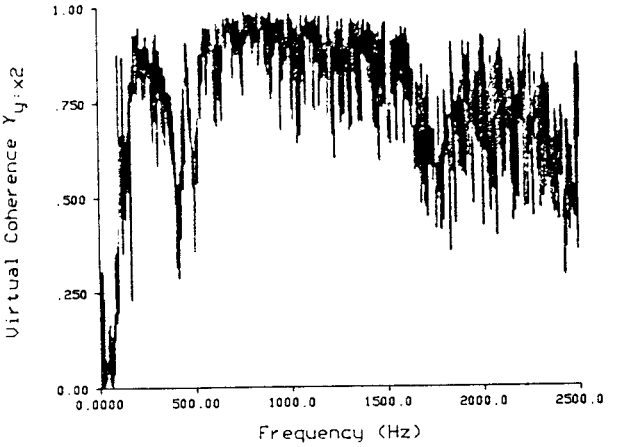

Figure 13. Virtual Coherence #2, Random Noise Test

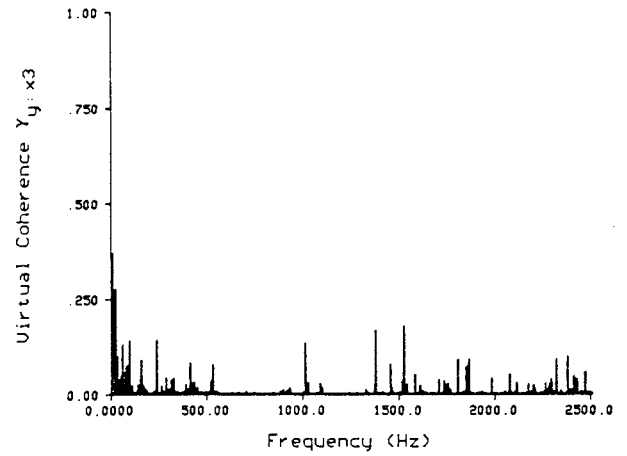

Figure 14. Virtual Coherence #3, Random Noise Test

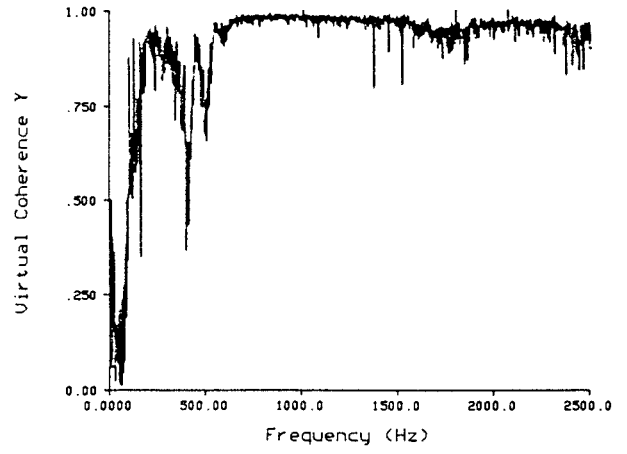

Figure 15. Total Coherence, Random Noise Test

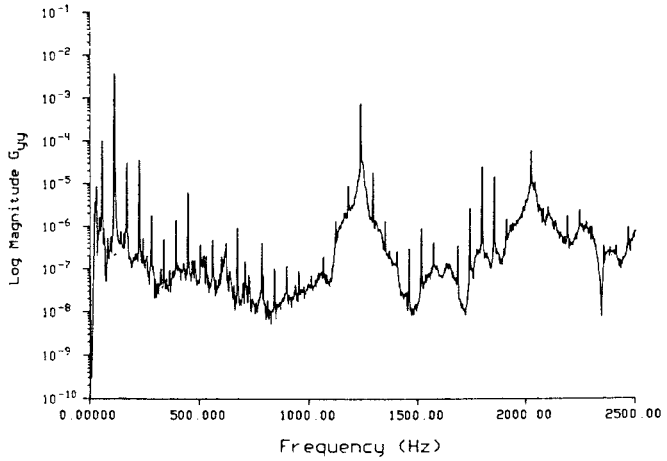

Figure 16. PSD of Measured Output, Compressor Test

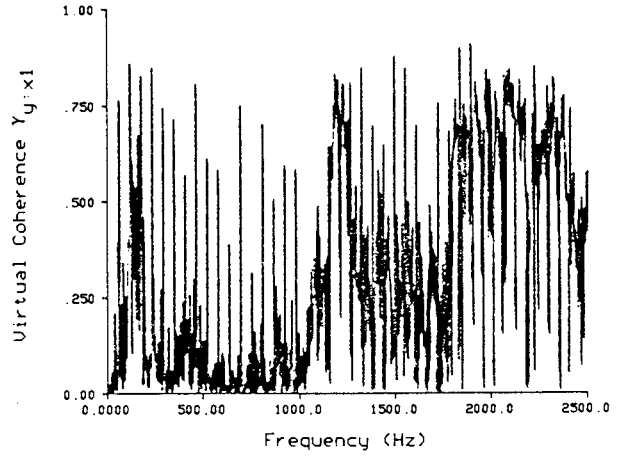

Figure 17. Virtual Coherence #1, Compressor Test

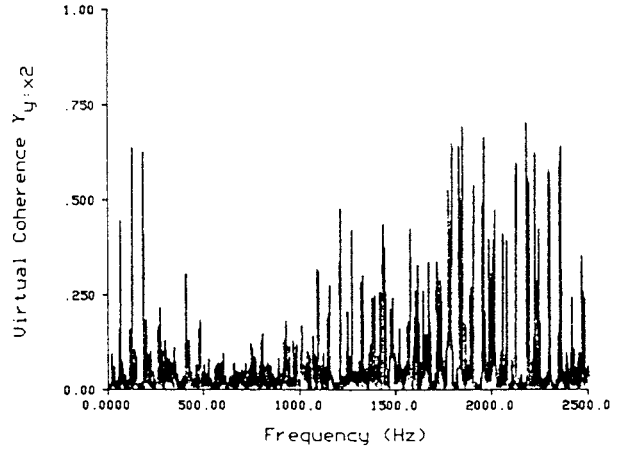

Figure 18. Virtual Coherence #2, Compressor Test

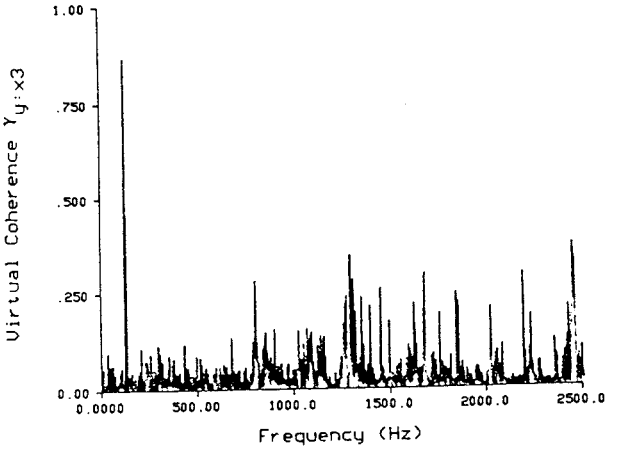

Figure 19. Virtual Coherence #3, Compressor Test

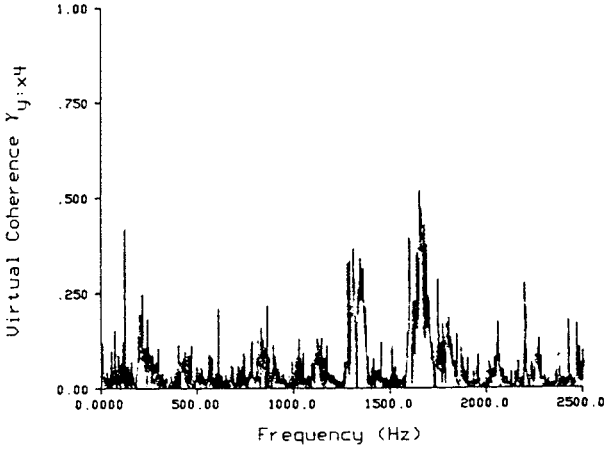

Figure 20. Virtual Coherence #4, Compressor Test

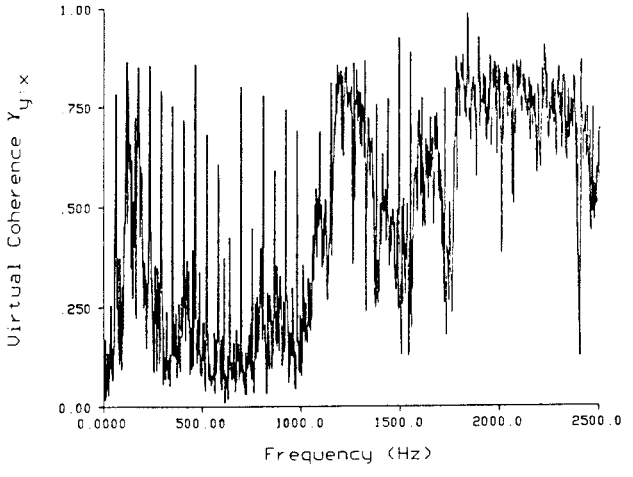

Figure 21. Total Coherence, Compressor Test